Commun. Comput. Phys.
doi: 10.4208/cicp.240315.301215a

Vol. **20**, No. 5, pp. 1340-1358
November 2016

# An Adaptive Grid Method for Singularly Perturbed Time-Dependent Convection-Diffusion Problems

Yanping Chen[1,*] and Li-Bin Liu[2]

[1] *School of Mathematical Sciences, South China Normal University, Guangzhou 510631, China.*
[2] *School of Mathematics and Computer, Chizhou University, Chizhou, Anhui 247000, China.*

Received 24 March 2015; Accepted (in revised version) 30 December 2015

**Abstract.** In this paper, we study the numerical solution of singularly perturbed time-dependent convection-diffusion problems. To solve these problems, the backward Euler method is first applied to discretize the time derivative on a uniform mesh, and the classical upwind finite difference scheme is used to approximate the spatial derivative on an arbitrary nonuniform grid. Then, in order to obtain an adaptive grid for all temporal levels, we construct a positive monitor function, which is similar to the arc-length monitor function. Furthermore, the $\varepsilon$-uniform convergence of the fully discrete scheme is derived for the numerical solution. Finally, some numerical results are given to support our theoretical results.

**AMS subject classifications**: 65L10, 65L12, 65L50

**Key words**: Uniform convergence, singularly perturbed, convection-diffusion problems, adaptive grid, an upwind finite difference scheme.

## 1 Introduction

In this paper, we consider the following singularly perturbed time-dependent convection-diffusion problem

$$\begin{cases} u_t(x,t)+\mathcal{L}_{x,\varepsilon}u(x,t)=f(x,t), & (x,t)\in G=\Omega\times(0,T]\equiv(0,1)\times(0,T], \\ u(x,0)=u_0(x), & x\in\Omega, \\ u(0,t)=u(1,t)=0, & t\in(0,T], \end{cases} \tag{1.1}$$

where

$$\mathcal{L}_{x,\varepsilon}u\equiv-\varepsilon u_{xx}+a(x)u_x+b(x)u,$$

*Corresponding author. *Email address:* yanpingchen@scnu.edu.cn (Y. Chen)

 ©2016 Global-Science Press

https://doi.org/10.4208/cicp.240315.301215a Published online by Cambridge University Press

$0<\varepsilon\ll 1$ is a small parameter. It is also assumed that $a(x)$ and $b(x)$ are sufficiently smooth functions, and there exist constants $\alpha$ and $\beta$ such that

$$a(x)\geq\alpha>0, \qquad b(x)\geq\beta\geq 0, \quad \forall x\in[0,1]. \tag{1.2}$$

Under conditions (1.2) and enough smoothness and compatibility conditions imposed on the functions $u_0(x)$ and $f(x,t)$, the above problem (1.1) has a unique solution which exhibits a boundary layer at $x=1$ (see, e.g. [1]).

Due to the presence of boundary layer, the classical finite difference or finite element methods will not give some satisfactory numerical results on an uniform mesh. Thus, in order to get a reliable numerical solution for (1.1) by using the classical numerical methods, an unacceptably large number of mesh points ($\varepsilon$-dependent) are required. Obviously, the amount of computation in this way is too huge. Therefore, many researchers tried to develop the concept of $\varepsilon$-uniform numerical methods, in which the order of convergence and the error constant are independent of $\varepsilon$.

In the past few decades, many $\varepsilon$-uniform numerical schemes were proposed in the literature for the singularly perturbed problems(see, e.g. [2]). As far as we know, the numerical methods for singularly perturbed problems are widely classified into two categories, namely, the layer-adapted grid approach and the adaptive grid approach. Of these two approaches, $\varepsilon$-uniform numerical results for the first approach is more satisfactory. For this reason, based on the layer-adapted grid approach, there have been some numerical results of the singularly perturbed time-dependent convection-diffusion problems (see, e.g. [3–10]). However, we know that the above layer-adapted grid approach must require a priori information about the location and width of the boundary layer. Obviously, if a priori information is unavailable about the boundary layer, the layer-adapted grid approach will become invalid. Thus, the adaptive grid approach is more popular in solving singularly perturbed problems.

Recently, Gowrisankar and Natesan [11] developed an adaptive grid approach to solve the above problem (1.1). However, on each time level, they must use an adaptive grid algorithm to obtain a non-uniform grid. In other words, they obtained a different spatial mesh on each time level. This drawback motivates to construct a non-uniform grid which is suitable for all time levels, in which the same order of convergence and the error estimation can be established. In [12], in order to obtain a mesh for all time levels, Gowrisankar and Natesan considered equidistribution of $u(x,t)$ at a fixed time $T_0$, $0<T_0\leq T$, where $u(x,t)$ is the solution of problem (1.1). Then, they used the classical upwind finite difference scheme on this mesh and obtained a first-order rate of convergence for the numerical method. In a word, the monitor functions presented in [11, 12] are much more complex. Therefore, it is always desirable to provide an efficient monitor function and the corresponding mesh generation algorithm in a simplest way.

In this paper, we will study an adaptive grid approach of problem (1.1). Specifically, we first use the backward Euler method on an uniform mesh to discrete the time derivative of problem (1.1). On each time level, we obtain a second-order singularly perturbed ordinary differential equation. Then, we can transform these equations into a system of

https://doi.org/10.4208/cicp.240315.301215a Published online by Cambridge University Press

singularly perturbed convection-diffusion equations, which is discreted by using classical upwind finite difference scheme on an arbitrary mesh. Finally, we will use some techniques proposed in [13] to obtain an adaptive grid for all time levels and study the optimal rate of convergence for the full discrete scheme of (1.1). It is noted that unlike the mesh given in [11,12] we obtain an adaptive grid for all time levels.

*Notation.* Throughout this paper we use $C$, sometimes subscripted, to denote a generic positive constant that is independent of the perturbation parameter $\varepsilon$ and mesh parameters $N$ and $M$. It may take different values in different place. $L_\infty(0,1)$ and $L_1(0,1)$ denote the usual Sobolev space with associated norms $\|\cdot\|_\infty$ and $\|\cdot\|_1$, respectively. For two real-value functions $v(x)$ and $V(x)$, the norm $\|v\|_{-1,\infty}=\min_{V:V'=v}\|V(x)\|_\infty$ will be used. For any vector-value function $\mathbf{g}=(g_1,\cdots,g_m)^T$, $g_i\in L_\infty(0,1)$ for all $i$, we set $\|\mathbf{g}\|_\infty=\max\{\|g_1\|_\infty,\cdots,\|g_m\|_\infty\}$, $\|\mathbf{g}\|_{-1,\infty}=\max\{\|g_1\|_{-1,\infty},\cdots,\|g_m\|_{-1,\infty}\}$.

## 2 The time semidiscretization

First, we divide the time domain $[0,T]$ into $M$ sub-intervals and obtain the equidistant mesh with uniform time step $\Delta t$ such that

$$S_t^M=\{t_n=n\Delta t,\ n=0,\cdots,M,\ \Delta t=T/M\}.$$

Then, by using the backward Euler method to discretize the time derivative of problem (1.1), we can obtain the following semi-discrete scheme

$$\begin{cases} u^0(x)=u(x,0)=u_0(x), \quad x\in\Omega, \\ u^{n+1}(x)+\Delta t\mathcal{L}_{x,\varepsilon}u^{n+1}(x)=u^n(x)+\Delta t f(x,t_{n+1}), \\ u^{n+1}(0)=u^{n+1}(1)=0, \end{cases} \tag{2.1}$$

where $u^n(x)$ is the semi-discrete approximation solution of $u(x,t)$ at time level $t_n=n\Delta t$.

Next, to analyze the uniform convergence of the solution of (2.1) to the analytic solution of (1.1), we introduce the following maximum principle result [11]

$$\|(I+\Delta t\mathcal{L}_{x,\varepsilon})^{-1}\|_\infty\le\frac{1}{1+\beta\Delta t}, \tag{2.2}$$

which ensures the stability of the scheme (2.1).

Let $e_{n+1}=u(x,t_{n+1})-u^{n+1}(x)$ be the local error of the time semi-discrete scheme (2.1), it follows from [3] that one can deduce the following consistency results.

**Lemma 2.1.** *Assume that*

$$\left|\frac{\partial^i}{\partial t^i}u(x,t)\right|\le C,\quad (x,t)\in[0,1]\times[0,T],\quad 0\le i\le 2.$$

*Then, we have*

$$\|e_{n+1}\|_\infty\le C(\Delta t)^2. \tag{2.3}$$

https://doi.org/10.4208/cicp.240315.301215a Published online by Cambridge University Press

Finally, from the above Lemma 2.1 and the stability result (2.2), we have the following convergence result.

**Theorem 2.1** ([11] Theorem 3.2)**.** *Under the hypothesis of Lemma* 2.1*, we obtain*

$$\sup_{n\leq T/\Delta t}\|u(x,t_n)-u^n(x)\|_\infty \leq C\Delta t. \tag{2.4}$$

Therefore, the semi-discrete scheme (2.1) is uniformly convergent of first-order in time.

# 3 The spatial discretization and adaptive spatial grids

## 3.1 Preliminary results

Here, we first rewrite scheme (2.1) as follows

$$\begin{cases} -\varepsilon u_{xx}^{n+1}(x)+a(x)u_x^{n+1}(x)+b(x)u^{n+1}(x)=g^n(x)+f(x,t_{n+1}), \quad x\in\Omega, \\ u^{n+1}(0)=u^{n+1}(1)=0, \\ u^0(x)=u(x,0)=u_0(x), \quad x\in\Omega, \end{cases} \tag{3.1}$$

where $g^n(x)=-\frac{u^{n+1}(x)-u^n(x)}{\Delta t}$.

Obviously, from the hypothesis condition of Lemma 2.1, and by using the Taylor series expansion, we have

$$|g^n(x)|\leq C, \quad x\in[0,1]. \tag{3.2}$$

Furthermore, the first equation of (3.1) can be written into the following system of equations

$$\begin{cases} -\varepsilon u_{xx}^1(x)+a(x)u_x^1(x)+b(x)u^1(x)=g^0(x)+f(x,t_1), \\ -\varepsilon u_{xx}^2(x)+a(x)u_x^2(x)+b(x)u^2(x)=g^1(x)+f(x,t_2), \\ \qquad\qquad\vdots \qquad\qquad \vdots \qquad\qquad \vdots \\ -\varepsilon u_{xx}^M(x)+a(x)u_x^M(x)+b(x)u^M(x)=g^{M-1}(x)+f(x,t_M). \end{cases} \tag{3.3}$$

Denote $u^j(x)=w_j(x)(j=1,\cdots,M)$, $\mathbf{w}(x)=(w_1(x),\cdots,w_M(x))^T$ and $\mathbf{F}(x)=(g^0(x)+f(x,t_1),\cdots,g^{M-1}(x)+f(x,t_M))^T$, combining the above equations (3.3) with initial boundary value conditions, we can obtain the following systems of coupled convection-diffusion problems

$$\begin{cases} \mathcal{L}\mathbf{w}(x):=-\varepsilon\mathbf{w}_{xx}(x)-A(x)\mathbf{w}_x(x)+B(x)\mathbf{w}(x)=\mathbf{F}(x), \quad x\in(0,1), \\ \mathbf{w}(0)=\mathbf{w}(1)=\mathbf{0}, \end{cases} \tag{3.4}$$

where $A(x)=\mathrm{diag}(-a(x))$ and $B(x)=\mathrm{diag}(b(x))$ are $M\times M$ diagonal matrixes, respectively.

https://doi.org/10.4208/cicp.240315.301215a Published online by Cambridge University Press

**Remark 3.1.** Since $A(x)$ is a diagonal matrix, the above problem (3.4) is called a weakly coupled convection-diffusion problem. Let $A_{ii}(x)$ and $B_{ii}(x)$ be the $i$th diagonal elements of $A(x)$ and $B(x)$, respectively. Then it follows from (1.2) that

$$\max_{x\in[0,1]} A_{ii}(x) = -\alpha < 0, \quad B_{ii}(x) > 0. \tag{3.5}$$

Next, the following theorem will give the stability analysis for the continuous problem (3.4).

**Theorem 3.1.** *Suppose* $\mathbf{w}$ *solves* (3.4). *Assume the functions* $A_{ii}(x)$, $B_{ii}(x)$ *satisfy* (3.5). *Then*

$$\|\mathbf{w}(x)\|_\infty \le C\|\mathbf{F}(x)\|_{-1,\infty}, \tag{3.6}$$

*where* $C$ *is a constant, independent of* $\varepsilon$ *and* $\Delta t$.

*Proof.* The proof is similar to Theorem 1 in [14]. □

**Corollary 3.1.** *Given* $\mathbf{s}\in L^2(0,1)$, $\mathbf{v}(x), \widetilde{\mathbf{v}}(x) \in H^1(0,1)$ *such that* $\mathbf{v}(0) = \widetilde{\mathbf{v}}(1)$ *and*

$$L\mathbf{v}(x) - L\widetilde{\mathbf{v}}(x) = \mathbf{s}(x).$$

*If* $\mathbf{S}'(x) = -\mathbf{s}(x)$, *where* $\mathbf{S}(x)$ *is a bound piecewise continuous function vector. Then*

$$\|\mathbf{v}(x) - \widetilde{\mathbf{v}}(x)\|_\infty \le C\|L\mathbf{v}(x) - L\widetilde{\mathbf{v}}(x)\|_{-1,\infty}.$$

**Remark 3.2.** There have been some results for layer-adapted approach to the solution of system of convection-diffusion problems (see, e.g. [15–17]). In [13], Liu and Chen developed a robust adaptive grid method to solve a system of two singularly perturbed convection-diffusion equations with weak coupling. Next, we will use some techniques developed in [13] to construct the numerical method of problem (3.4).

### 3.2 Finite difference scheme

In this subsection, we discretize (3.4) by means of a first-order upwind scheme on the following non-uniform spatial mesh

$$\Omega^N = \{0 = x_0 < x_1 < \cdots < x_N = 1\}$$

with the spatial step size $h_i := x_i - x_{i-1} (i = 1, \cdots, N)$. Before constructing the upwind finite difference scheme of (3.4), for a mesh function $\{v_i\}_{i=0}^N$, define the difference operators as follows

$$D^- v_i = \frac{v_i - v_{i-1}}{h_i}, \quad Dv_i = \frac{v_{i+1} - v_i}{\hbar_i},$$

where $\hbar_i = (h_i + h_{i+1})/2$.

https://doi.org/10.4208/cicp.240315.301215a Published online by Cambridge University Press

Then, on $\Omega^N$, the simple upwind finite difference spatial discretization of (3.4) takes the form

$$\begin{cases} -\varepsilon DD^-\mathbf{W}_i - A_iD^-\mathbf{W}_i + B_i\mathbf{W}_i = \mathbf{F}_i, \\ \mathbf{W}_0 = \mathbf{W}_N = \mathbf{0}, \end{cases} \tag{3.7}$$

where $\mathbf{W}_i = (W_{1,i},\cdots,W_{M,i})^T$ is the numerical solution of exact solution $\mathbf{w}(x_i)$, $A_i = A(x_i)$, $B_i = B(x_i)$ and $\mathbf{F}_i = \mathbf{F}(x_i)$.

First, in order to give the stability property of the discretization (3.7), we define the discrete norms as follows

$$\|v\|_{\infty,\overline{\Omega}_x^N} := \max_{i=0,\cdots,N}|v_i|, \quad \|v\|_{1,\overline{\Omega}_x^N} := \sum_{i=0}^{N-1} h_{i+1}|v_i|, \quad \|v\|_{-1,\infty,\overline{\Omega}_x^N} := \min_{V:V_x=v}\|V\|_{\infty,\overline{\Omega}_x^N}.$$

For vector-valued function $\mathbf{v}$ set

$$\|\mathbf{v}\|_{\infty,\overline{\Omega}_x^N} := \max_{j=1,\cdots,M}\|v_j\|_{\infty,\overline{\Omega}_x^N}, \quad \|\mathbf{v}\|_{1,\overline{\Omega}_x^N} := \max_{j=1,\cdots,M}\|v_j\|_{1,\overline{\Omega}_x^N},$$
$$\|\mathbf{v}\|_{-1,\infty,\overline{\Omega}_x^N} := \max_{j=1,\cdots,M}\|v\|_{-1,\infty,\overline{\Omega}_x^N}.$$

Then, the discrete maximum principle implies the following stability property of the discretization (3.7).

**Lemma 3.1.** *Let $\mathbf{W}_i = (W_{1,i},\cdots,W_{M,i})^T$ be the solution of discretization (3.7), $i = 1,\cdots,N$. Then we have*

$$\|\mathbf{W}\|_{\infty,\overline{\Omega}_x^N} \le C. \tag{3.8}$$

*Proof.* For each $j(1 \le j \le M)$, it follows from (3.7) that

$$-\varepsilon DD^-W_{j,i} - (-a(x_i))D^-W_{j,i} + b(x_i)W_{j,i} = g^{j-1}(x_i) + f(x_i,t_j). \tag{3.9}$$

Furthermore, the discrete maximum principle implies the following standard stability result

$$\begin{aligned} \|\mathbf{W}^j\|_{\infty,\overline{\Omega}_x^N} &\le C\|\mathbf{g}^{j-1} + \mathbf{f}^j\|_{\infty,\overline{\Omega}_x^N} \\ &\le C\|\mathbf{g}^{j-1}\|_{\infty,\overline{\Omega}_x^N} + \|\mathbf{f}^j\|_{\infty,\overline{\Omega}_x^N}, \end{aligned} \tag{3.10}$$

where $\mathbf{g}^{j-1} = (g^{j-1}(x_1),\cdots,g^{j-1}(x_N))^T$, $\mathbf{f}^j = (f(x_1,t_j),\cdots,f(x_N,t_j))^T$.

Using the notion of vector, the desired estimate (3.8) follows from (3.2), (3.10) and the continuity condition of function $f(x,t)$. □

https://doi.org/10.4208/cicp.240315.301215a Published online by Cambridge University Press

### 3.3 Mesh generation algorithm

A commonly used method to construct such a grid is the use of a positive monitor function $\overline{M}(x)$ and the equidistribution principle. The grid $\Omega^N=\{x_j|0=x_0<x_1<\cdots<x_N=1\}$ is chosen such that

$$\int_{x_{i-1}}^{x_i}\overline{M}(s)ds=\frac{1}{N}\int_0^1\overline{M}(s)ds,\quad i=1,\cdots,N. \tag{3.11}$$

So far, for a single singularly perturbed problem, the monitor function resulting a first order uniform convergence is the arc-length function $\overline{M}(x)=\sqrt{1+[u'(x)]^2}$ or its discrete analogue [18–23], where $u(x)$ is the exact solution of the singularly perturbed problem.

Recently, Liu and Chen [13] developed an adaptive grid approach to solve a system of two singularly perturbed convection-diffusion equations. Here, in this paper, similar to [13], we construct the following monitor function

$$\widetilde{M}(x)=\sqrt{1+\max_{x\in[0,1]}\left\{[\widetilde{W}_1'(x)]^2,\cdots,[\widetilde{W}_M'(x)]^2\right\}}, \tag{3.12}$$

where $\widetilde{W}_j(x)$ is the piecewise linear interpolant function passing through knots $(x_i,W_{j,i})$, $j=1,\cdots,M$, $i=1,\cdots,N$. Then, we can obtain a mesh which satisfies the following equation

$$\int_{x_{i-1}}^{x_i}\widetilde{M}(s)ds=\frac{1}{N}\int_0^1\widetilde{M}(s)ds. \tag{3.13}$$

In order to solve above equation (3.13), we construct the following iteration algorithm:

*Step 1.* Take $k=0$. Take the uniform mesh $\{x_i^{(0)}=i/N\}_{i=0}^N$ as the initial mesh for the iteration. Choose a constant $C_0>1$ that controls when the algorithm has to be terminated.

*Step 2.* Compute the numerical solution $\{W_{j,i}^{(k)}\}$ satisfying (3.1) on $\{x_i^{(k)}\}$. Set $h_i^{(k)}=x_i^{(k)}-x_{i-1}^{(k)}$ for each $i$. Let

$$l_i^{(k)}=h_i^{(k)}\sqrt{1+\max_{1\le j\le M}\left[\left(D^-W_{j,i}^{(k)}\right)^2\right]}=\sqrt{\left(h_i^{(k)}\right)^2+\max_{1\le j\le M}\left[\left(W_{j,i}^{(k)}-W_{j,i-1}^{(k)}\right)^2\right]}$$

be the max arc-length between the points $(x_{i-1}^{(k)},W_{j,i-1}^{(k)})$ and $(x_i^{(k)},W_{j,i}^{(k)})$, where $j=1,\cdots,M$. Then the total max arc-length can be written as

$$\begin{aligned}L^{(k)}&=\sum_{i=1}^N l_i^{(k)}=\sum_{i=1}^N h_i^{(k)}\sqrt{1+\max_{1\le j\le M}\left[\left(D^-W_{j,i}^{(k)}\right)^2\right]}\\&=\sum_{i=1}^N\sqrt{\left(h_i^{(k)}\right)^2+\max_{1\le j\le M}\left[\left(W_{j,i}^{(k)}-W_{j,i-1}^{(k)}\right)^2\right]}.\end{aligned}$$

https://doi.org/10.4208/cicp.240315.301215a Published online by Cambridge University Press

*Step 3.* If the stopping criterion

$$\frac{\max\limits_{1\le i\le N}\left\{l_i^{(k)}\right\}}{L^{(k)}}\le\frac{C_0}{N} \tag{3.14}$$

holds true, then go to Step 5. Otherwise, continue to Step 4.

*Step 4.* Generate the new mesh by equidistributing arc-length of current computed solution: Choose points $\{x_0^{(k+1)}<x_1^{(k+1)}<\cdots<x_N^{(k+1)}\}$ such that

$$\int_{x_{i-1}^{(k+1)}}^{x_i^{(k+1)}}\sqrt{1+\max_{x\in[0,1]}\left\{\left[\left(\widetilde{W}_1^k(x)\right)'\right]^2,\cdots,\left[\left(\widetilde{W}_M^k(x)\right)'\right]^2\right\}}=L^{(k)}/N,$$

where $i=1,2,\cdots,N$.

*Step 5.* Set $k=k+1$, return to Step 2.

*Step 6.* Take $\{x_i^{(k)}\}$ as the final mesh and calculate the corresponding solution $\{W_{j,i}^{(k)}\}$, then stop.

# 4 Error estimate

## 4.1 First-order a posteriori error estimate

In this section, we first give the following result which is a direct extension of Corollary 3.1.

**Corollary 4.1.** *Let* $\mathbf{w}(x)$ *be the solution of* (3.4), $\widetilde{\mathbf{W}}(x)=\left(\widetilde{W}_1'(x),\cdots,\widetilde{W}_M'(x)\right)^T$ *be piecewise linear interpolant function vector. Then we have*

$$\|\mathbf{w}(x)-\widetilde{\mathbf{W}}(x)\|_\infty\le C\|L\mathbf{w}(x)-L\widetilde{\mathbf{W}}(x)\|_{-1,\infty,\overline{\Omega}_x^N}. \tag{4.1}$$

Next, based on Lemma 3.1 and Corollary 4.1, we can give the maximum norm a posteriori error estimate for the numerical scheme (3.7).

**Theorem 4.1.** *Let* $\mathbf{w}(x)$ *be the solution of* (3.4), $\mathbf{W}_i$ *be the solution of* (3.7) *on an arbitrary nonuniform mesh* $\Omega^N$ *and* $\widetilde{\mathbf{W}}(x)$ *be piecewise linear interpolant function vector to the solution* $\mathbf{W}$ *of* (3.7). *Then we have*

$$\|\widetilde{\mathbf{W}}(x)-\mathbf{w}(x)\|_\infty\le C\left\{\max_{1\le i\le N}h_i\left[\max_{1\le j\le M}\left|D^-W_{j,i}\right|\right]+\max_{1\le i\le N}h_i\right\}. \tag{4.2}$$

*Proof.* The proof is similar to Theorem 3.1 in [13]. □

https://doi.org/10.4208/cicp.240315.301215a Published online by Cambridge University Press

### 4.2 Accuracy of the fully discretised solution

Next, we consider the adaptive mesh generated by (3.13). We recall that

$$l_i = h_i\sqrt{1+\max_{1\le j\le M}\left[\left(D^- W_{j,i}\right)^2\right]} = \sqrt{(h_i)^2+\max_{1\le j\le M}\left[\left(W_{j,i}-W_{j,i-1}\right)^2\right]} \tag{4.3}$$

is the max arc-length between the points $\left(x_{i-1},W_{j,i-1}\right)$ and $\left(x_i,W_{j,i}\right)$, where $j=1,\cdots,M$. Then the total max arc-length $L^N$ can be written as

$$L^N = \sum_{i=1}^{N} l_i = \sum_{i=1}^{N} h_i\sqrt{1+\max_{1\le j\le M}\left[\left(D^- W_{j,i}\right)^2\right]}. \tag{4.4}$$

It is obvious that

$$L^N \ge \sum_{i=1}^{N} h_i = 1.$$

From (3.7), we have

$$-\varepsilon DD^- W_{j,i} + a_i D^- W_{j,i} + b_i W_{j,i} = g^{j-1}(x_i) + f(x_i,t_j), \tag{4.5}$$

$$W_{j,0} = W_{j,N} = 0, \tag{4.6}$$

where $i=1,\cdots,N$, $j=1,\cdots,M$.

Let $G^j_{k,i} = G^j(x_k,\xi_i)$ be the discrete Green's function, where $x_k,\xi_j \in \overline{\Omega}^N_x$. Then we have

$$W_{j,k} = \sum_{i=1}^{N-1} \hbar_i G^j_{k,i}\left[g^{j-1}(x_i) + f(x_i,t_j)\right]. \tag{4.7}$$

Similar to [20], we can obtain the following properties for the discrete Green's function.

$$0 \le G^j_{k,i} \le \frac{2}{\alpha} \quad \text{for} \quad 1\le k,i\le N-1, \tag{4.8}$$

$$\sum_{k=1}^{N}\left|G^j_{k,i} - G^j_{k,i-1}\right| \le \frac{4}{\alpha}, \tag{4.9}$$

where $j=1,\cdots,M$.

With the above preparations, we are now ready to upper-bound the arc-length $L^N$.

**Lemma 4.1.** *Let $\{W_{j,k}\}_{k=0}^N$ $(j=1,\cdots,M)$ be the solution computed by our scheme (3.7) on an adaptive mesh $\{x_k\}_{k=0}^N$ produced by (3.13). Then*

$$\sum_{k=1}^{N}|W_{j,k}-W_{j,k-1}| \le C, \quad j=1,\cdots,M, \tag{4.10}$$

*where $C$ is a constant, independent of the parameters $\varepsilon$.*

https://doi.org/10.4208/cicp.240315.301215a Published online by Cambridge University Press

*Proof.* From (4.7), we have

$$W_{j,k}=\sum_{i=1}^{N-1}\hbar_i G_{k,i}^j\left[g^{j-1}(x_i)+f(x_i,t_j)\right], \tag{4.11}$$

$$W_{j,k-1}=\sum_{i=1}^{N-1}\hbar_i G_{k-1,i}^j\left[g^{j-1}(x_i)+f(x_i,t_j)\right]. \tag{4.12}$$

Furthermore, we obtain

$$\begin{aligned}\sum_{k=1}^{N}|W_{j,k}-W_{j,k-1}|&=\sum_{i=1}^{N-1}\hbar_i\left|G_{k,i}^j-G_{k-1,i}^j\right|\left|g^{j-1}(x_i)+f(x_i,t_j)\right|\\&\le\sum_{i=1}^{N-1}\hbar_i\left|G_{k,i}^j-G_{k-1,i}^j\right|\left(\left|g^{j-1}(x_i)\right|+|f(x_i,t_j)|\right).\end{aligned} \tag{4.13}$$

The desired estimate (4.10) follows from (3.2), (4.9) and the condition of $f(x,t)$. □

Based on Lemma 4.1, we can get the upper-bound of $L^N$.

**Lemma 4.2.** *The total max arc-length $L^N$, defined by (4.4), satisfies the following estimate:*

$$L^N\le C. \tag{4.14}$$

*Proof.* Since

$$\begin{aligned}L^N&=\sum_{i=1}^{N}h_i\sqrt{1+\max_{1\le j\le M}\left[\left(D^-W_{j,i}\right)^2\right]}\le\sum_{i=1}^{N}h_i\left(1+\max_{1\le j\le M}\left|D^-W_{j,i}\right|\right)\\&=1+\max_{1\le j\le M}\sum_{i=1}^{N}\left|W_{j,i}-W_{j,i-1}\right|.\end{aligned} \tag{4.15}$$

The desired estimate (4.14) follows from Lemma 4.1. □

**Corollary 4.2.** *Let $\{x_i\}_{i=0}^N$ be any mesh generated by the algorithm. Then we have*

$$h_i\le CN^{-1}. \tag{4.16}$$

*Proof.* The proof can be seen in [20] (Corollary 4.1). □

Finally, we establish the optimal first-order convergence of the upwind scheme (3.7) uniformly in the perturbation parameter $\varepsilon$.

**Theorem 4.2.** *Let $\mathbf{w}(x)$ be the solution of (3.4), $\mathbf{W}_i$ be the solution of (3.7) on a mesh $\{x_i\}_{i=0}^N$ that satisfies (3.13) and $\widetilde{\mathbf{W}}(x)$ be piecewise linear interpolant function vector. Then we have*

$$\max_{1\le j\le M}\max_{0\le i\le N}|w_j(x_i)-W_{j,i}|\le CN^{-1}, \tag{4.17}$$

*where $C$ is a constant independent of $\varepsilon$, $N$ and $M$.*

https://doi.org/10.4208/cicp.240315.301215a Published online by Cambridge University Press

*Proof.* Using Theorem 4.1, Corollary 4.2 and Lemma 4.2 gives for $1\leq i\leq N$,

$$\begin{aligned}\max_{1\leq j\leq M}\max_{0\leq i\leq N}|w_j(x_i)-W_{j,i}| &\leq \|\widetilde{\mathbf{W}}(x)-\mathbf{w}(x)\|_\infty\\ &\leq C\left[\max_{1\leq i\leq N}h_i\max_{1\leq j\leq M}\left|D^-W_{j,i}\right|+\max_{1\leq i\leq N}h_i\right]\\ &\leq C\max_{1\leq i\leq N}h_i\sqrt{1+\max_{1\leq j\leq M}\left\{\left(D^-W_{j,i}\right)^2\right\}}+C\max_{1\leq i\leq N}h_i\\ &\leq C\max_{1\leq i\leq N}l_i^N+C\max_{1\leq i\leq N}h_i\\ &=C\frac{L^N}{N}+C\max_{1\leq i\leq N}h_i\\ &\leq CN^{-1}. \end{aligned}\tag{4.18}$$

This completes the proof of this theorem. □

**Corollary 4.3.** *If we take $N^{-q}\leq C\Delta t$ with $0<q<1$, then from (4.17), we have*

$$\max_{1\leq j\leq M}\max_{0\leq i\leq N}|w_j(x_i)-W_{j,i}|\leq C\Delta tN^{-1+q}.\tag{4.19}$$

Finally, we establish the $\varepsilon$-uniform convergence of the fully discrete scheme (3.7) on the adaptive grid obtained through monitor function given in (3.12).

**Theorem 4.3.** *Let $u(x_i,t_j)$ be the exact solution of problem (1.1) and $W_{j,i}$ be the discrete solution of the fully discrete scheme (3.7) at time level $t_j=j\Delta t$. Assume that $N^{-q}\leq C\Delta t$ with $0<q<1$. Then, the error associated with the fully discrete scheme (3.7) satisfies*

$$\max_{1\leq j\leq M}\max_{0\leq i\leq N}|u(x_i,t_j)-W_{j,i}|\leq C(\Delta t+N^{-1+q}).\tag{4.20}$$

*Proof.* The proof is similar to Theorem 4.7 in [11]. □

## 5 Numerical experiments and discussion

In this section, we shall present the numerical results obtained by the proposed adaptive grid method to confirm the theoretical results. It is well known that the constant $C_0$ in the above mesh generation algorithm gives an intimation of how close we are from the equidistribution of the monitor function. Here, we take $C_0=1.2$ in all our numerical results. Moreover, in all the tables, we begin with $N=32$ and the time step $\Delta t=0.1$, and we multiply $N$ by two and divide $\Delta t$ by two.

Consider the following time-dependent convection-diffusion problem:

$$\begin{cases} u_t(x,t)-\varepsilon u_{xx}(x,t)+(1+x(1-x))u_x(x,t)=f(x,t), & (x,t)\in(0,1)\times(0,1],\\ u(x,0)=u_0(x), & 0<x<1,\\ u(0,t)=u(1,t)=0, & t\in[0,1]. \end{cases}\tag{5.1}$$

https://doi.org/10.4208/cicp.240315.301215a Published online by Cambridge University Press

We choose the initial data $u_0(x)$ and the source term $f(x,t)$ to fit with the analytical solution

$$u(x,t)=\exp(-t)(\exp(-1/\varepsilon)+(1-\exp(-1/\varepsilon))x-\exp(-(1-x)/\varepsilon)).$$

Since the exact solution of this problem is known, we use the following formula (5.2) to calculate the maximum point-wise error

$$E_\varepsilon^{N,\Delta t}=\max_{0\le i\le N}\max_{0\le n\le M}|u(x_i,t_n)-U_i^n|, \tag{5.2}$$

where $u(x_i,t_n)$ and $U_i^n$ respectively, represent the exact and the numerical solution obtained on the mesh with $N$ intervals in the spatial direction and $M$ mesh intervals in the time direction, and $\Delta t=\frac{T}{M}$ is the uniform time step. The corresponding rate of convergence is given by

$$r_\varepsilon^{N,\Delta t}=\log_2\left(\frac{E_\varepsilon^{N,\Delta t}}{E_\varepsilon^{2N,\Delta t/2}}\right). \tag{5.3}$$

Firstly, based on the above definitions, the maximum point-wise errors and the corresponding order of convergence are given in Tables 1-2, respectively. It can be seen from these results that the numerical method presented in this paper converges uniformly in

Table 1: Maximum error calculated by using the presented method.

| $\varepsilon$ | Number of intervals $N$/time size $\Delta t$ | | | | |
|---|---|---|---|---|---|
| | $32/\frac{1}{10}$ | $64/\frac{1}{20}$ | $128/\frac{1}{40}$ | $256/\frac{1}{80}$ | $512/\frac{1}{160}$ |
| $10^0$ | 6.8921e-04 | 3.7085e-04 | 1.9290e-04 | 9.8440e-05 | 4.9739e-05 |
| $10^{-2}$ | 7.1532e-02 | 4.5000e-02 | 2.6393e-02 | 1.4579e-02 | 7.1423e-03 |
| $10^{-4}$ | 9.3382e-02 | 5.5430e-02 | 3.9185e-02 | 2.1997e-02 | 1.1787e-02 |
| $10^{-6}$ | 9.7044e-02 | 6.0392e-02 | 3.8509e-02 | 1.8888e-02 | 1.1989e-02 |
| $10^{-8}$ | 9.7889e-02 | 5.9632e-02 | 3.9439e-02 | 2.0684e-02 | 1.2039e-02 |

Table 2: Rate of convergence calculated by using the presented method.

| $\varepsilon$ | Number of intervals $N$/time size $\Delta t$ | | | |
|---|---|---|---|---|
| | $32/\frac{1}{10}$ | $64/\frac{1}{20}$ | $128/\frac{1}{40}$ | $256/\frac{1}{80}$ |
| $10^0$ | 0.8941 | 0.9430 | 0.9705 | 0.9849 |
| $10^{-2}$ | 0.6687 | 0.7698 | 0.8563 | 1.0294 |
| $10^{-4}$ | 0.7525 | 0.5004 | 0.8330 | 0.9001 |
| $10^{-6}$ | 0.6843 | 0.6492 | 1.0280 | 0.6558 |
| $10^{-8}$ | 0.7150 | 0.5965 | 0.9311 | 0.7808 |

https://doi.org/10.4208/cicp.240315.301215a Published online by Cambridge University Press

Table 3: The number of iterations by using the presented method.

| $\varepsilon$ | Number of intervals $N$/time size $\Delta t$ | | | | |
|---|---|---|---|---|---|
| | $32/\frac{1}{10}$ | $64/\frac{1}{20}$ | $128/\frac{1}{40}$ | $256/\frac{1}{80}$ | $512/\frac{1}{160}$ |
| $10^0$ | 1 | 1 | 1 | 1 | 1 |
| $10^{-2}$ | 3 | 3 | 3 | 3 | 2 |
| $10^{-4}$ | 5 | 8 | 4 | 6 | 6 |
| $10^{-6}$ | 11 | 10 | 6 | 4 | 11 |
| $10^{-8}$ | 21 | 14 | 18 | 8 | 12 |

Table 4: Maximum error calculated by using the Shishkin mesh.

| $\varepsilon$ | Number of intervals $N$/time size $\Delta t$ | | | | |
|---|---|---|---|---|---|
| | $32/\frac{1}{10}$ | $64/\frac{1}{20}$ | $128/\frac{1}{40}$ | $256/\frac{1}{80}$ | $512/\frac{1}{160}$ |
| $10^0$ | 6.8921e-04 | 3.7085e-04 | 1.9290e-04 | 9.8440e-05 | 4.9737e-05 |
| $10^{-2}$ | 5.5988e-02 | 3.8931e-02 | 2.4826e-02 | 1.4919e-02 | 8.6489e-03 |
| $10^{-4}$ | 6.4187e-02 | 4.3984e-02 | 2.7665e-02 | 1.6409e-02 | 9.4977e-03 |
| $10^{-6}$ | 6.4292e-02 | 4.4129e-02 | 2.7833e-02 | 1.6608e-02 | 9.5732e-03 |
| $10^{-8}$ | 6.4293e-02 | 4.4130e-02 | 2.7834e-02 | 1.6610e-02 | 9.5755e-03 |

Table 5: Rate of convergence calculated by using the Shishkin mesh.

| $\varepsilon$ | Number of intervals $N$/time size $\Delta t$ | | | |
|---|---|---|---|---|
| | $32/\frac{1}{10}$ | $64/\frac{1}{20}$ | $128/\frac{1}{40}$ | $256/\frac{1}{80}$ |
| $10^0$ | 0.8941 | 0.9430 | 0.9705 | 0.9849 |
| $10^{-2}$ | 0.5242 | 0.6491 | 0.7346 | 0.7866 |
| $10^{-4}$ | 0.5453 | 0.6689 | 0.7536 | 0.7889 |
| $10^{-6}$ | 0.5429 | 0.6649 | 0.7449 | 0.7948 |
| $10^{-8}$ | 0.5429 | 0.6649 | 0.7448 | 0.7947 |

the maximum point-wise errors with first-order accuracy. For each $\varepsilon$, $N$ and $M$, Table 3 also lists the number of iterations $K$ required by the above mesh generation algorithm. We can see that the number of iterations are very small, even for $\varepsilon \ll 1$.

In addition, in order to illustrate the advantages of our new method, we also calculate some numerical results for the well-known layer-adapted meshes, Shishkin mesh and Bakhvalov mesh, which are listed in Tables 4-7. It is noted that these results come from [11]. More information about the Shishkin mesh and the Bakhvalov mesh can be found in [1, 2]. From the results of Tables 1-6, we get a conclusion that the maximum point-wise errors and the corresponding rate of convergence calculated on our adaptive grid are almost the same to that calculated on Bakhvalov mesh, but the rate of convergence of

https://doi.org/10.4208/cicp.240315.301215a Published online by Cambridge University Press

Table 6: Maximum error calculated by using the Bakhvalov mesh.

| | Number of intervals $N$/time size $\Delta t$ | | | | |
|---|---|---|---|---|---|
| $\varepsilon$ | $32/\frac{1}{10}$ | $64/\frac{1}{20}$ | $128/\frac{1}{40}$ | $256/\frac{1}{80}$ | $512/\frac{1}{160}$ |
| $10^0$ | 6.8921e-04 | 3.7085e-04 | 1.9290e-04 | 9.8440e-05 | 4.9739e-05 |
| $10^{-2}$ | 3.6778e-02 | 2.2324e-02 | 1.2953e-02 | 7.2482e-03 | 3.9080e-03 |
| $10^{-4}$ | 6.6889e-02 | 3.7859e-02 | 2.0136e-02 | 1.0334e-02 | 5.2851e-03 |
| $10^{-6}$ | 7.3993e-02 | 4.2358e-02 | 2.2715e-02 | 1.1750e-02 | 5.9784e-03 |
| $10^{-8}$ | 7.6146e-02 | 4.3468e-02 | 2.3305e-02 | 1.2073e-02 | 6.1429e-03 |

Table 7: Rate of convergence calculated by using the Bakhvalov mesh.

| | Number of intervals $N$/time size $\Delta t$ | | | |
|---|---|---|---|---|
| $\varepsilon$ | $32/\frac{1}{10}$ | $64/\frac{1}{20}$ | $128/\frac{1}{40}$ | $256/\frac{1}{80}$ |
| $10^0$ | 0.8941 | 0.9430 | 0.9705 | 0.9849 |
| $10^{-2}$ | 0.7203 | 0.7853 | 0.8376 | 0.8912 |
| $10^{-4}$ | 0.8211 | 0.9108 | 0.9624 | 0.9674 |
| $10^{-6}$ | 0.8048 | 0.8990 | 0.9509 | 0.9749 |
| $10^{-8}$ | 0.8088 | 0.8993 | 0.9489 | 0.9748 |

the numerical solution calculated on our adaptive grid is higher than that calculated on Shishkin mesh.

Further, we calculate the normalized flux by

$$F_\varepsilon u(x,t)=\varepsilon\frac{\partial u(x,t)}{\partial x}, \tag{5.4}$$

and we use the following formula to represent its numerical approximation

$$F_\varepsilon^N U_i^n=\varepsilon D^- U_i^n. \tag{5.5}$$

The errors in the normalized flux can be given as

$$D_\varepsilon^{N,\Delta t}=\max_{0\le i\le N}\max_{0\le n\le M}|F_\varepsilon u(x_i,t_n)-F_\varepsilon^N U_i^n| \tag{5.6}$$

and the corresponding order of convergence is determined from

$$q_\varepsilon^{N,\Delta t}=\log_2\left(\frac{D_\varepsilon^{N,\Delta t}}{D_\varepsilon^{2N,\Delta t/2}}\right). \tag{5.7}$$

Similarly, the maximum point-wise errors of the normalized flux and its order of convergence are listed in Tables 8-9. Again, we can see the $\varepsilon$-uniform first-order convergence of the maximum point-wise errors of the normalized flux.

https://doi.org/10.4208/cicp.240315.301215a Published online by Cambridge University Press

Table 8: Maximum point-wise error of the normalized flux.

| | Number of intervals $N$/time size $\Delta t$ | | | | |
|---|---|---|---|---|---|
| $\varepsilon$ | $32/\frac{1}{10}$ | $64/\frac{1}{20}$ | $128/\frac{1}{40}$ | $256/\frac{1}{80}$ | $512/\frac{1}{160}$ |
| $10^{0}$ | 1.7039e-02 | 8.8121e-03 | 4.4877e-03 | 2.2670e-03 | 1.1392e-03 |
| $10^{-2}$ | 1.4029e-01 | 8.4302e-02 | 4.7918e-02 | 2.5968e-02 | 1.3154e-02 |
| $10^{-4}$ | 1.7140e-01 | 1.0052e-01 | 6.4661e-02 | 3.5685e-02 | 1.8861e-02 |
| $10^{-6}$ | 1.7690e-01 | 1.0693e-01 | 6.3921e-02 | 3.2955e-02 | 1.9098e-02 |
| $10^{-8}$ | 1.7709e-01 | 1.0598e-01 | 6.5570e-02 | 3.4214e-02 | 1.9154e-02 |

Table 9: Rate of convergence of the normalized flux.

| | Number of intervals $N$/time size $\Delta t$ | | | |
|---|---|---|---|---|
| $\varepsilon$ | $32/\frac{1}{10}$ | $64/\frac{1}{20}$ | $128/\frac{1}{40}$ | $256/\frac{1}{80}$ |
| $10^{0}$ | 0.9512 | 0.9735 | 0.9852 | 0.9927 |
| $10^{-2}$ | 0.7348 | 0.8150 | 0.8838 | 0.9812 |
| $10^{-4}$ | 0.7699 | 0.6377 | 0.8576 | 0.9199 |
| $10^{-6}$ | 0.7263 | 0.7423 | 0.9558 | 0.7871 |
| $10^{-8}$ | 0.7407 | 0.6927 | 0.9384 | 0.8369 |

The comparison of numerical solution and exact solution are plotted in Fig. 1 for $N=64$, $\Delta t=1/64$ and $\varepsilon=10^{-10}$. Fig. 2 also lists the comparison of numerical solution and exact solution at different time levels. It is shown from Figs. 1-2 that the numerical solution can approximate the exact solution very well. In addition, to make the reader understanding of the meshes computed by the above algorithm when solving problem (5.1), Fig. 3 shows the mesh movement after each iteration. It is worth noting that Fig. 3 should be read from bottom to top. The left of this figure is labeled with the value of $C_0$ for which the stopping criterion (3.14) becomes an equation. It can be seen from Fig. 3 that taking any smaller value of $C_0$ will increase the number of iterations. As a complement of our theoretical results, the loglog plots of maximum point-wise error of solution $E_{\varepsilon}^{N,\Delta t}$ and the normalized flux $D_{\varepsilon}^{N,\Delta t}$ are given in Figs. 4-5, respectively, which demonstrate the fact of first-order uniform convergence of the presented adaptive grid method.

In summary, our numerical results confirm our theoretical results.

## 6 Conclusion

In this paper, we have discussed an adaptive grid approach for the singularly perturbed time-dependent convection-diffusion problem (1.1). We first apply the backward-Euler scheme to discretize the problem (1.1) with respect to time derivative and the upwind finite difference scheme on an non-uniform mesh to approximate the spatial derivative.

https://doi.org/10.4208/cicp.240315.301215a Published online by Cambridge University Press

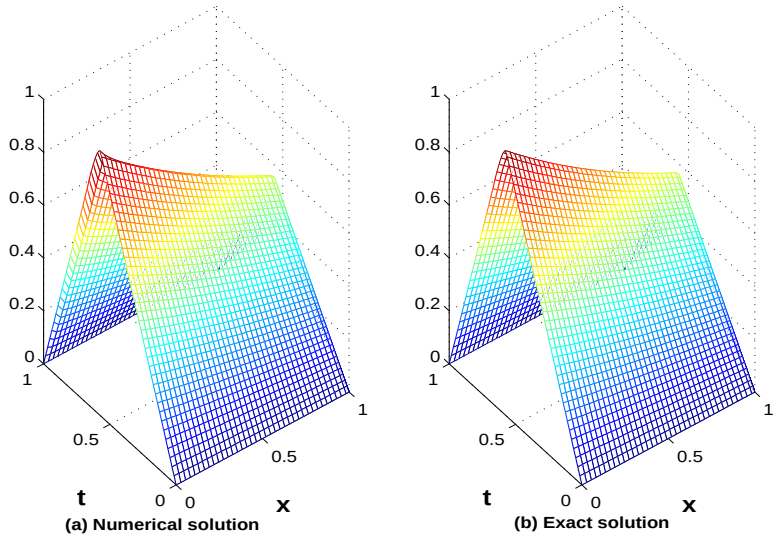



Figure 1: The comparison of numerical solution and exact solution for $N=64$, $\Delta t=1/64$ and $\varepsilon=10^{-10}$.

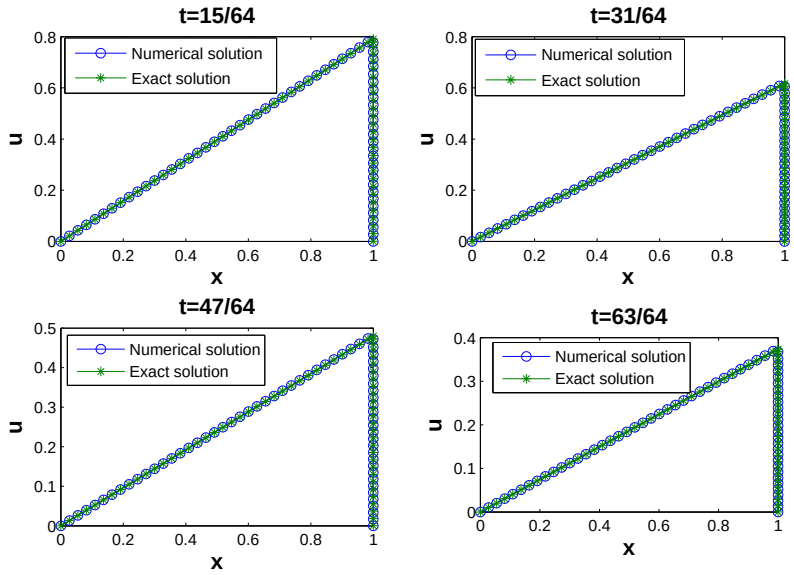



Figure 2: The comparison of numerical solution and exact solution at different time levels for $N=64$, $\Delta t=1/64$ and $\varepsilon=10^{-10}$.

Then, in order to obtain an adaptive spatial grid at every time level, we construct a positive monitor function given in (3.12), and design a mesh generation algorithm. Similar to [13], an a posteriori error estimate for the proposed numerical scheme is obtained. We also establish that the presented adaptive grid approach is of first-order rate of conver-

https://doi.org/10.4208/cicp.240315.301215a Published online by Cambridge University Press

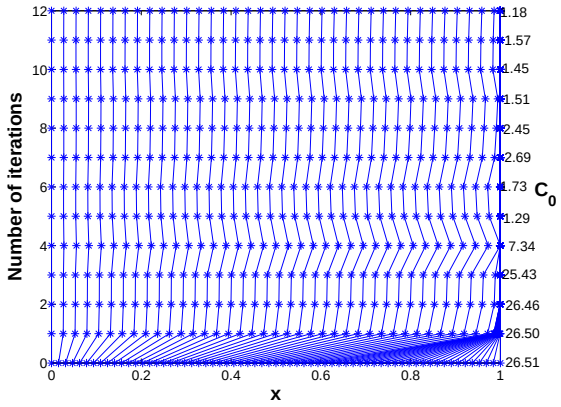



Figure 3: Mesh movement for $\varepsilon=10^{-7}$, $N=64$ and $\Delta t=1/20$.

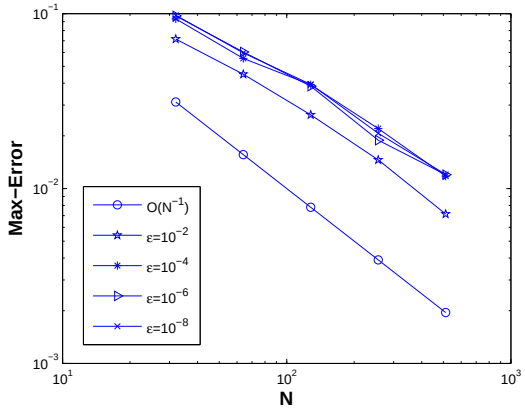



Figure 4: Loglog plot of the maximum point-wise error of the solution $E_\varepsilon^{N,\Delta t}$.

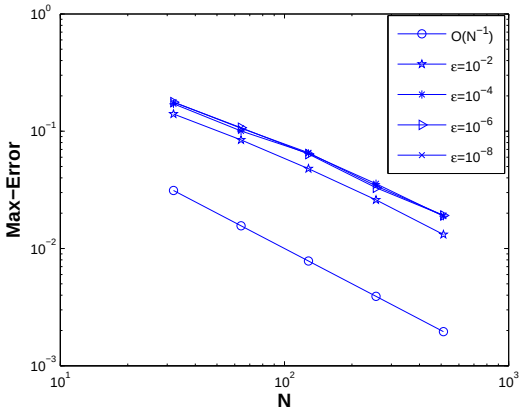



Figure 5: Loglog plot of the maximum point-wise error of the normalized flux $D_\varepsilon^{N,\Delta t}$.

https://doi.org/10.4208/cicp.240315.301215a Published online by Cambridge University Press

gence in both the spatial and temporal variables. Finally, some numerical results are conducted to support the theoretical results and also, to demonstrate the effectiveness of the adaptive spatial grid obtained by the above mesh generation algorithm. It is also shown from the numerical results that the proposed numerical method has a better numerical accuracy compared to the layer adaptive grid method. We point out that the adaptive grid method used in this work can be extended to other type of singularly perturbed time-dependent problems.

In addition, we think that the mesh generation algorithm proposed in this paper can also extend to higher dimensional singularly perturbed problems. Taking two dimensional singularly perturbed convection-diffusion problems as an example, we first may obtain an uniform mesh for the $x$ direction, then use the mesh generation algorithm presented in this paper to produce the non-uniform mesh in $y$ direction. At last, we use the similar technique to obtain the non-uniform mesh in $x$ direction. Thus, in the future work, we will consider the adaptive grid approach for the higher dimensional singularly perturbed problems.

## Acknowledgments

This work is supported by National Science Foundation of China (91430104, 11271145, 11301044, 11671157), and the key projects of Excellent young talents fund in universities of Anhui province (2013SQRL095ZD).

### References

[1] H. G. Roos, M. Stynes, L. Tobiska, Numerical methods for singularly perturbed differential equations. Spring, Berlin, 1996.
[2] J. J. H. Miller, E.O'Riordan, G.I. Shishkin, Fitted numercial methods for singularly perturbation problems, World Scientific, Singapore, 1996.
[3] C. Clavero, J. C. Jorge, F. Lisbona, A uniformly convergent scheme on a nonuniform mesh for convection-diffusion parabolic problems, Journal of Computational and Applied Mathematics, 154 (2003) 415-429.
[4] K. Mukherjee, S. Natesan, Parameter-uniform hybird numerical scheme for time-dependent convection-dominated initial-boundary-value problems, Computing, 84 (2009) 209-230.
[5] K. Mukherjee, S. Natesan, Richardson extrapolation technique for singularly perturbed parabolic convection-diffsion problems, Computing, 92 (2011) 1-32.
[6] M. K. Kadalbajoo, A. Awasthi, A parameter uniform difference scheme for singularly perturbed parabolic problem in one space dimension, Applied Mathematicas and Computation, 183 (2006) 42-60.
[7] C. Clavero, J. L. Gracia, M. Stynes, A simple analysis of a hybird numerical method for time-dependent convection-diffusion problems, Journal of Computational and Applied Mathematics, 235 (2011) 5240-5248.
[8] V. Gupta, M. K. Kadalbajoo, A layer adaptive B-spline collocation method for singularly perutrbed one-dimensional parabolic problem with a boundary turning point, Numerical Methods Partial Differential Equation, 27 (2011) 1143-1164.

https://doi.org/10.4208/cicp.240315.301215a Published online by Cambridge University Press

[9] E. O'Riordan, M. L. Pickett, G. I. Shishkin, Parameter-uniform finite difference schemes for singularly perturbed parabolic diffusion-convection-reaction problems, Mathematics of Computation, 75 (2006) 1135-1154.
[10] A. Jha, M.K. Kadalbajoo, A robust layer adapted difference method for singularly perturbed two-parameter parabolic problems, Internation Journal of Computer Mathematics, 92 (2015) 1204-1221.
[11] S. Gowrisankar, S. Natesan, Uniformly convergent numerical method for singularly perturbed parabolic initial-boundary-value problems with equidistributed grids, International Journal of Computer Mathematics, 91 (2014) 553-577.
[12] S. Gowrisankar, S. Natesan, Robust numerical scheme for singularly perturbed convection-diffusion parabolic initial-boundary-value problems on equidistributed grids, Computer Physics Communications, 185 (2014) 2008-2019.
[13] L.-B. Liu, Y. Chen, A robust adaptive grid method for a system of two singularly perturbed Convection-diffusion equations with weak coupling, Journal of Scientific Computing, 61 (2014) 1-16.
[14] T. Linß, Analysis of a system of singularly perturbed convection-diffusion equations with strong coupling, SIAM Journal on Numerical Analysis, 47 (2009) 1847-1862.
[15] Z. D. Cen, Parameter-uniform finite difference scheme for a system of coupled singularly perturbed convection-diffusion equations, International Journal of Computer Mathematics, 82 (2005) 177-192.
[16] H.-G. Roos, C. Reibiger, Numerical analysis of a system of singularly perturbed convection-diffusion equations related to optimal control, Numerical Mathematics: Theory, Methods and Applications, 4 (2011) 562-575.
[17] T. Linß, Dresden, Analysis of an upwind finite-difference scheme for a system of coupled singularly perturbed convection-diffusion equations, Computing, 79 (2007) 23-32.
[18] Y. Qiu, D.M. Sloan, T. Tang, Convergence analysis of an adaptive finite difference method for a singular perturbation problem, Journal of Computational and Applied Mathematics, 116 (2000) 121-143.
[19] N. Kopteva, Maximum norm a posteriori error estimates for a one-dimensional convection-diffusion problem, SIAM Journal on Numerical Analysis, 39 (2001) 423-441.
[20] N. Kopteva, M. Stynes, A robust adaptive method for quasi-linear one-dimensional convection-diffusion problem, SIAM Journal on Numerical Analysis, 39 (2001) 1446-1467.
[21] Y. Chen, Uniform pointwise convergence for a singularly perturbed problem using arc-length equidistribution,Journal of Computational and Applied Mathematics, 159 (2003) 25-34.
[22] Y. Chen, Uniform convergence analysis of finite difference approximations for singular perturbation problems on an adapted grid, Advances in Computational Mathematics, 24 (2006) 197-212.
[23] J. Mackenzie, Uniform convergence analysis of an upwind finite difference approximation of a convection-diffusion bondary value problem on an adaptive gird, IMA Journal of Numerical Analysis, 19 (1999) 233-249.

https://doi.org/10.4208/cicp.240315.301215a Published online by Cambridge University Press